

Toward the Rational Design of Supramolecular Coordination Polymers. The Effect of Solvent and Substituent Changes on the Structure of Self-Assembled Metal-Organometallic Networks

Moonhyun Oh,* Gene B. Carpenter, and D. A. Sweigart*

Department of Chemistry, Brown University, Providence, Rhode Island 02912

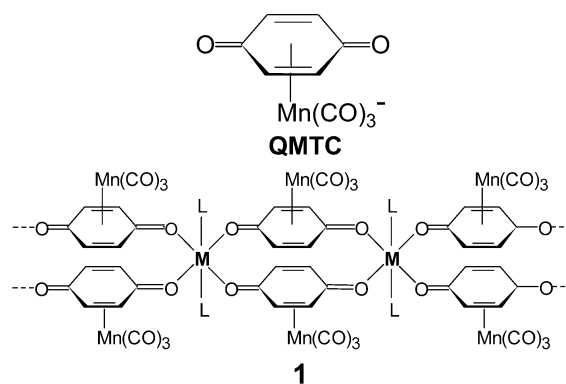
Received April 9, 2003

Summary: Self-assembly of the π -complex (η^4 -benzoquinone) $Mn(CO)_3^-$ (**QMTC**) with metal ions [$Mn(II)$, $Co(II)$, $Zn(II)$] generates neutral metal-organometallic coordination networks (MOMNs). The network architecture can be controlled by (1) a solvent-induced change in coordination geometry at the metal nodes and (2) the introduction of substituents on the benzoquinone ring.

Metal-coordination-directed formation of both discrete^{1,2} and infinite^{1,3–6} metal-organic supramolecular networks (MONs) has attracted much recent attention. The driving force behind this work is the desire to construct functional solids that have applications in areas such as catalysis, sensing, guest–host chemistry, optics, and magnetics. A significant limitation on this chemistry is a generally poor ability to control or even predict the network architecture that will result when the modular components are combined. This difficulty in predicting structure is often due to the existence of supramolecular isomers of similar energies.⁴ Even when a particular structural architecture can be predesigned with some confidence, the product often consists of several interpenetrating networks, which usually, but not always,⁶ limits the ability of the material to bind potential substrates. It is clear that improvements in the ability to rationally design supramolecular networks

will require a better understanding of the factors that control structure.

We recently reported^{7–9} the construction of metal-organometallic networks (MOMNs) that utilize metal ions (or metal ion clusters) as nodes linked by the organometallic ligand **QMTC**. This η^4 -benzoquinone complex serves as a bifunctional spacer by binding to the metal nodes via both quinone oxygen atoms. In DMSO solvent, divalent metal ions Mn^{2+} , Co^{2+} , Ni^{2+} , and Cd^{2+} react with **QMTC** to generate the neutral one-dimensional quinonoid polymers **1**. Each metal ion node in **1**



(1) (a) Lehn, J. M. *Supramolecular Chemistry: Concepts and Perspectives*; VCH: Weinheim, 1995. (b) Steed, J. W.; Atwood, J. L. *Supramolecular Chemistry*; Wiley: Chichester, 2000.

(2) (a) Philp, D.; Stoddart, J. F. *Angew. Chem., Int. Ed.* **1996**, *35*, 1154. (b) Leininger, S.; Olenyuk, B.; Stang, P. J. *Chem. Rev.* **2000**, *100*, 853. (c) Holliday, B. J.; Mirkin, C. A. *Angew. Chem., Int. Ed.* **2001**, *40*, 2022. (d) Fujita, M. *Chem. Soc. Rev.* **1998**, *27*, 417. (e) MacGillivray, L. R.; Groeneman, R. H.; Atwood, J. L. *J. Am. Chem. Soc.* **1998**, *120*, 2676. (f) Cho, Y. L.; Uh, H.; Chang, S.-Y.; Chang, H.-Y.; Choi, M.-G.; Shin, I.; Jeong, K.-S. *J. Am. Chem. Soc.* **2001**, *123*, 1258.

(3) (a) Batten, S. R.; Robson, R. *Angew. Chem., Int. Ed.* **1998**, *37*, 1460. (b) Robson, R. *J. Chem. Soc., Dalton Trans.* **2000**, 3735. (c) Eddaoudi, M.; Moler, D. B.; Li, H.; Chen, B.; Reineke, T. M.; O'Keeffe, M.; Yaghi, O. M. *Acc. Chem. Res.* **2001**, *34*, 319. (d) Evans, O. R.; Lin, W. *Acc. Chem. Res.* **2002**, *35*, 511.

(4) Moulton, B.; Zaworotko, M. J. *Chem. Rev.* **2001**, *101*, 1629.

(5) (a) Bourne, S. A.; Lu, J.; Mondal, A.; Moulton, B.; Zaworotko, M. J. *Angew. Chem., Int. Ed.* **2001**, *40*, 2111. (b) Abourahma, H.; Moulton, B.; Kravtsov, V.; Zaworotko, M. J. *J. Am. Chem. Soc.* **2002**, *124*, 9990. (c) Chen, B.; Eddaoudi, M.; Hyde, S. T.; O'Keeffe, M.; Yaghi, O. M. *Science* **2001**, *291*, 1021. (d) Dong, Y.-B.; Layland, R. C.; Pschirer, N. G.; Smith, M. D.; Bunz, U. H. F.; zur Loye, H.-C. *Chem. Mater.* **1999**, *11*, 1413. (e) Choi, H. J.; Suh, M. P. *J. Am. Chem. Soc.* **1998**, *120*, 10622. (f) Biradha, K.; Fujita, M. *J. Chem. Soc., Dalton Trans.* **2000**, 3805. (g) Biradha, K.; Fujita, M. *Angew. Chem., Int. Ed.* **2002**, *41*, 3392. (h) Cui, Y.; Evans, O. R.; Ngo, H. L.; White, P. S.; Lin, W. *Angew. Chem., Int. Ed.* **2002**, *41*, 1159. (i) Evans, O. R.; Lin, W. *Chem. Mater.* **2001**, *13*, 3009.

(6) Rosi, N. L.; Eddaoudi, M.; Kim, J.; O'Keeffe, M.; Yaghi, O. M. *Angew. Chem., Int. Ed.* **2002**, *41*, 284.

has octahedral geometry, with solvent DMSO providing two axial ligands L. Analogous two-dimensional quinonoid coordination networks, again with octahedral nodes, can also be generated in DMSO under certain experimental conditions.⁹ In this communication, we show that a change in solvent and/or introduction of substituents on the carbocyclic ring in **QMTC** can have a profound effect on the architecture of the resulting coordination network. Significantly, the variations seen are easily understood and hence predictable.

In the reaction of **QMTC** with Mn^{2+} and Co^{2+} , it was found that changing from DMSO to the less coordinating solvent MeOH leads to the formation of 3-D diamondoid structures in which the metal ion nodes adopt tetrahedral rather than octahedral^{7,9} coordination. The metal ions are coordinated to the quinone oxygen atoms only

(7) Oh, M.; Carpenter, G. B.; Sweigart, D. A. *Angew. Chem., Int. Ed.* **2001**, *40*, 3191.

(8) (a) Oh, M.; Carpenter, G. B.; Sweigart, D. A. *Chem. Commun.* **2002**, 2168. (b) Oh, M.; Carpenter, G. B.; Sweigart, D. A. *Organometallics* **2002**, *21*, 1290. (c) Oh, M.; Carpenter, G. B.; Sweigart, D. A. *Angew. Chem., Int. Ed.*, in press.

(9) Oh, M.; Carpenter, G. B.; Sweigart, D. A. *Angew. Chem., Int. Ed.* **2002**, *41*, 3650.

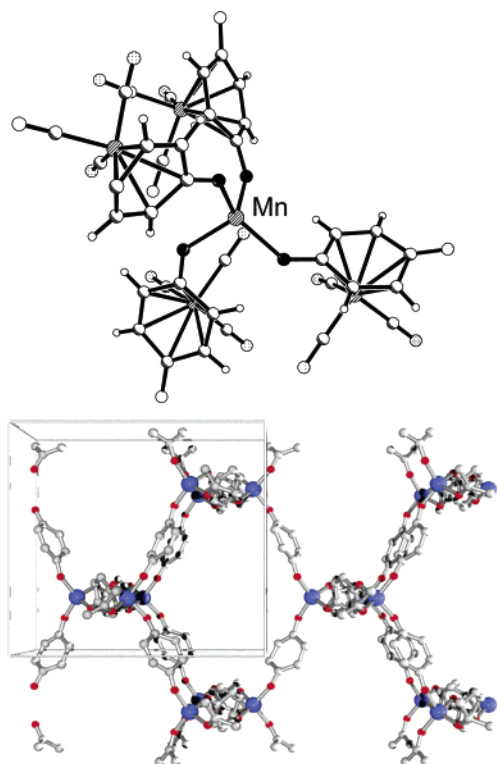


Figure 1. Tetrahedral geometry at a node in $[\text{Mn}(\text{QMTC})_2]_\infty$ and one of the two interpenetrated 3-D diamondoid networks in the associated polymer (with $\text{Mn}(\text{CO})_3$ groups not shown).

and no solvent is incorporated into the coordination polymers.¹⁰ Figure 1 shows the geometry around one of the Mn^{2+} nodes in $[\text{Mn}(\text{QMTC})_2]_\infty$.¹¹ The polymers $[\text{Co}(\text{QMTC})_2]_\infty$ and $[\text{Zn}(\text{QMTC})_2]_\infty$, obtained from MeOH solvent, also feature tetrahedral coordination and possess overall structures virtually identical to that found for $[\text{Mn}(\text{QMTC})_2]_\infty$.¹² All three structures consist of two interpenetrating 3-D diamondoid networks, one of which is illustrated in Figure 1 for $[\text{Mn}(\text{QMTC})_2]_\infty$. Thus, it is concluded that in the case of Mn^{2+} and Co^{2+} , switching the solvent from DMSO to MeOH results in a fundamental change in architecture that is triggered by a

(10) $[\text{M}(\text{QMTC})_2]_\infty$ ($\text{M} = \text{Mn}, \text{Co}, \text{Zn}$) were synthesized by combining (η^5 -semiquinone) $\text{Mn}(\text{CO})_3^{\text{sb}}$ (20 mg, 0.08 mmol) and $\text{M}(\text{OAc})_2$ (10 mg, 0.04 mmol) in 1.0 mL of MeOH. The biphasic mixture was sealed and heated to 75 °C for 1 day. During this period, the reaction mixture became homogeneous and crystals of product slowly deposited in ca. 80% yield. The product was washed with MeOH and Et_2O and then air-dried. For $[\text{Mn}(\text{QMTC})_2]_\infty$: IR (KBr) ν_{CO} 2027 (s), 1961 (s), 1932 (s), 1922 (s), 1570 (s), 1555 (m), 1510 (s) cm^{-1} . Anal. Calcd for $\text{C}_{18}\text{H}_8\text{Mn}_3\text{O}_{10}$: C, 39.38; H, 1.47. Found: C, 39.11; H, 1.53. For $[\text{Co}(\text{QMTC})_2]_\infty$: IR (KBr) ν_{CO} 2035 (s), 1981 (m), 1972 (m), 1936 (s), 1575 (m), 1557 (m), 1502 (s) cm^{-1} . Anal. Calcd for $\text{C}_{18}\text{H}_8\text{CoMn}_2\text{O}_{10}$: C, 39.09; H, 1.46. Found: C, 38.93; H, 1.20. The $[\text{Zn}(\text{QMTC})_2]_\infty$ obtained was found to be identical with that obtained from DMSO solvent and previously reported.⁷

(11) Crystal data for $[\text{Mn}(\text{QMTC})_2]_\infty$: formula $\text{C}_{36}\text{H}_{16}\text{Mn}_6\text{O}_{20}$, fw = 1098.13, tetragonal, space group $P4_3$, $a = 15.8914(8)$ Å, $b = 15.8914(8)$ Å, $c = 15.3532(14)$ Å, $V = 3877.2(4)$ Å³, $Z = 4$, $\rho_{\text{calcd}} = 1.881$ g cm^{-3} , $\mu = 1.980$ mm⁻¹, $F(000) = 2168$, θ range 2.25–26.42°, 559 variables refined with 7937 independent reflections to final R indices [$I > 2\sigma(I)$] of $R_1 = 0.0574$ and $wR_2 = 0.1478$, and GOF = 1.141. X-ray data collection utilized Mo $K\alpha$ radiation at 298 K with a CCD area detector.

(12) Crystal data for $[\text{Co}(\text{QMTC})_2]_\infty$: formula $\text{C}_{36}\text{H}_{16}\text{Co}_2\text{Mn}_4\text{O}_{20}$, fw = 1106.10, tetragonal, space group $P4_3$, $a = 15.742(2)$ Å, $b = 15.742(2)$ Å, $c = 15.405(3)$ Å, $V = 3817.5(10)$ Å³, $Z = 4$, $\rho_{\text{calcd}} = 1.925$ g cm^{-3} , $\mu = 2.219$ mm⁻¹, $F(000) = 2184$, θ range 2.26–26.41°, 559 variables refined with 7792 independent reflections to final R indices [$I > 2\sigma(I)$] of $R_1 = 0.0706$ and $wR_2 = 0.1718$, and GOF = 1.102. Unit cell determinations showed that the structure of $[\text{Zn}(\text{QMTC})_2]_\infty$ was identical to the polymer grown from DMSO and previously reported.⁷

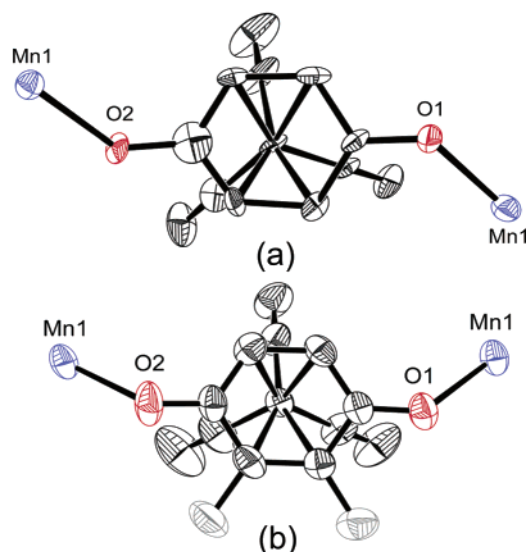


Figure 2. Bonding of the quinone oxygens to $\text{Mn}(\text{II})$ nodes in (a) $[\text{Mn}(\text{QMTC})_2]_\infty$ and (b) $[\text{Mn}(2,3\text{-Me}_2\text{QMTC})_2]_\infty$.

change from octahedral to tetrahedral coordination at the divalent metal ion node. This change in geometry, which is likely due to the generally weaker coordinating ability of MeOH compared to DMSO, is suggestive of a potentially useful methodology for controlling and predicting coordination network architecture. In contrast to the behavior seen with Mn^{2+} and Co^{2+} , the polymer obtained with Zn^{2+} has the tetrahedral diamondoid structure whether the solvent is MeOH or DMSO.⁷ This fact reflects the greater tendency for Zn^{2+} to assume a tetrahedral geometry.

The quinone rings in $[\text{M}(\text{QMTC})_2]_\infty$ ($\text{M} = \text{Mn}, \text{Co}, \text{Zn}$) adopt a slightly bowed conformation, with the oxygen atoms being bent about 10° out of the carbocyclic diene plane. As a consequence, the $\text{Mn}(\text{CO})_3$ moiety is much more weakly bonded to the oxygen-bearing carbon atoms than to the diene carbons, meaning that the bonding is effectively of the η^4 type. Figure 2a gives a view normal to one of the quinone rings in $[\text{Mn}(\text{QMTC})_2]_\infty$. An essentially identical picture holds for the cobalt and zinc analogues. It may be seen in Figure 2a that the bonding from a given quinone to the metal nodes occurs in a *trans*-manner from the oxygen lone pairs. In other words, the lone pairs would appear to be stereochemically active (*vide infra*).

The introduction of methyl groups at the 2- and 3-positions of the benzoquinone ring was found to greatly influence the manner in which the quinone oxygen lone pairs bind to the metal nodes. Crystal structure analysis of coordination polymers $[\text{M}(2,3\text{-Me}_2\text{QMTC})_2]_\infty$ ($\text{M} = \text{Mn}^{2+}, \text{Zn}^{2+}$) grown in MeOH or EtOH solvent revealed that in each case it is the lone pairs projecting away from the methyls that bind to the nodes, resulting in the *cis*-arrangement illustrated in Figure 2b.^{13,14} Presumably, this bonding pattern is dictated by the steric requirements of the methyl groups. In any event, the stereochemical switch from the *trans* to *cis* results in a concomitant change in the polymer architecture from a 2-fold interpenetrated 3-D diamondoid structure (Figure 1) to a noninterpenetrated ruffled 2-D rhombohedral grid (Figure 3). Despite the *trans* to *cis* and diamondoid to rhombohedral structural changes, the metal nodes in $[\text{M}(2,3\text{-Me}_2\text{QMTC})_2]_\infty$ remain tetra-

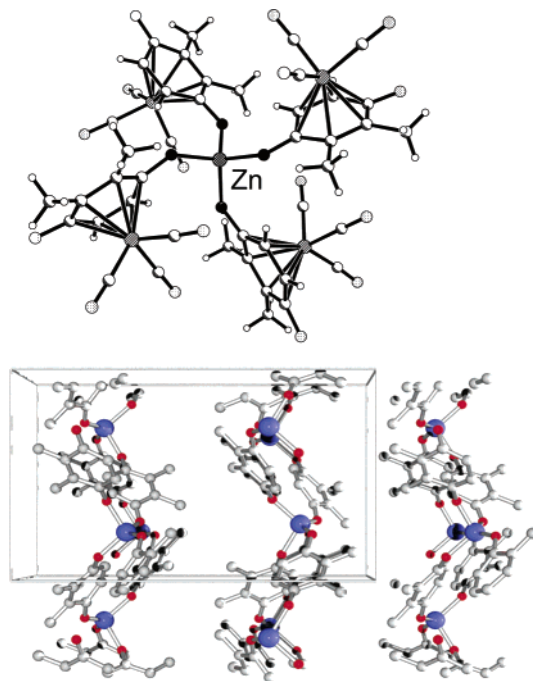


Figure 3. Tetrahedral geometry at a node in $[\text{Zn}(2,3\text{-Me}_2\text{-QMTC})_2]_\infty$ and the 2-D rhombohedral network in the associated polymer (with $\text{Mn}(\text{CO})_3$ groups not shown).

hedrally bonded to the quinone oxygens, as is shown in Figure 3 for $[\text{Zn}(2,3\text{-Me}_2\text{-QMTC})_2]_\infty$.

The 3-D diamondoid and 2-D ruffled grid networks were obtained by the same experimental procedure, except that 2,3-Me₂QMTC replaced QMTC in the latter. The quinone ring in $[\text{M}(2,3\text{-Me}_2\text{-QMTC})_2]_\infty$ is slightly bowed as in $[\text{M}(\text{QMTC})_2]_\infty$, and the bonding to $\text{Mn}(\text{CO})_3$ is best described as η^4 . In $[\text{Zn}(2,3\text{-Me}_2\text{-QMTC})_2]_\infty$ the O–Zn–O angles span the narrow range of 108–111°, indicating very little distortion from tetrahedral geometry. The polymer $[\text{Mn}(2,3\text{-Me}_2\text{-QMTC})_2]_\infty$ was crystallized from both MeOH and EtOH. The two structures are qualitatively similar, with the

(13) $[\text{M}(2,3\text{-Me}_2\text{-QMTC})_2]_\infty$ (M = Zn, Mn) were synthesized by combining (η^5 -2,3-dimethylseminquinone) $\text{Mn}(\text{CO})_3^{\text{sb}}$ (20 mg, 0.08 mmol) and $\text{M}(\text{OAc})_2$ (10 mg, 0.04 mmol) in 1.0 mL of MeOH. The biphasic mixture was sealed and heated to 80 °C for 1 day. During this period, the reaction mixture became homogeneous and crystals of product slowly deposited in ca. 85% yield. For $[\text{Zn}(\text{QMTC})_2]_\infty$: IR (KBr) ν_{CO} 2028 (s), 1947 (s, br), 1545 (m), 1503 (s), cm^{-1} . Anal. Calcd for $\text{C}_{22}\text{H}_{16}\text{-ZnMn}_2\text{O}_{10}$: C, 42.92; H, 2.62. Found: C, 42.78; H, 2.53. For $[\text{Mn}(2,3\text{-Me}_2\text{-QMTC})_2 \cdot \text{MeOH}]_\infty$: IR (KBr) ν_{CO} 2021 (s), 1954 (s), 1944 (s), 1942 (m), 1496 (m), cm^{-1} . Anal. Calcd for $\text{C}_{23}\text{H}_{20}\text{Mn}_3\text{O}_{11}$: C, 43.35; H, 3.16. Found: C, 43.22; H, 3.05. Heating (η^5 -2,3-dimethylseminquinone) $\text{Mn}(\text{CO})_3$ in EtOH produced $[\text{Mn}(2,3\text{-Me}_2\text{-QMTC})_2]_\infty$, as verified by X-ray diffraction (vide supra).

only notable difference being the incorporation of a molecule of MeOH in the former. The MeOH molecule was found to be weakly associated with the Mn^{2+} node ($\text{Mn}-\text{O} = 2.36 \text{ \AA}$), which produces some distortion in the O(quinone)–Mn–O(quinone) angles (range 97–111°). When $[\text{Mn}(2,3\text{-Me}_2\text{-QMTC})_2]_\infty$ is grown from EtOH, no solvent was found to be incorporated into the structure and the O–Mn–O angles are more nearly tetrahedral.

In summary, we have demonstrated that the gross architecture of metal-organometallic coordination networks (MOMNs) consisting of metal ion nodes linked by (η^4 -benzoquinone) $\text{Mn}(\text{CO})_3^-$ organometallogand spacers can be controlled by (1) a solvent-induced change in coordination geometry at the metal ion nodes from octahedral to tetrahedral and (2) a substituent-induced change in the stereochemistry of spacer binding to the nodes, resulting in the network switching from a 3-D interpenetrated diamondoid to a 2-D rhombohedral structure. Significantly, these simple changes are easily understood and, therefore, may find general utility in the rational design of supramolecular coordination networks.

Acknowledgment is made to the donors of the Petroleum Research Fund, administered by the American Chemical Society, for support of this work.

Supporting Information Available: X-ray crystallographic data for $[\text{Mn}(\text{QMTC})_2]_\infty$, $[\text{Mn}(2,3\text{-Me}_2\text{-QMTC})_2 \cdot \text{MeOH}]_\infty$, $[\text{Zn}(2,3\text{-Me}_2\text{-QMTC})_2]_\infty$, $[\text{Co}(\text{QMTC})_2]_\infty$, and $[\text{Mn}(2,3\text{-Me}_2\text{-QMTC})_2]_\infty$, respectively. This material is available free of charge via the Internet at <http://pubs.acs.org>. These files have also been deposited with the Cambridge Crystallographic Data Centre as registry numbers CCDC-204130, 204131, 204132, 204133, and 204134, respectively.

OM0302600

(14) Crystal data for $[\text{Zn}(2,3\text{-Me}_2\text{-QMTC})_2]_\infty$: formula $\text{C}_{22}\text{H}_{16}\text{ZnMn}_2\text{O}_{10}$, fw = 615.60, orthorhombic, space group $P2_12_12_1$, $a = 11.1472(6) \text{ \AA}$, $b = 11.8026(7) \text{ \AA}$, $c = 18.3879(10) \text{ \AA}$, $V = 2419.2(2) \text{ \AA}^3$, $Z = 4$, $\rho_{\text{calcd}} = 1.690 \text{ g cm}^{-3}$, $\mu = 2.065 \text{ mm}^{-1}$, $F(000) = 1232$, θ range 2.05–25.05°, 320 variables refined with 4268 independent reflections to final R indices [$I > 2\sigma(I)$] of $R_1 = 0.0479$ and $wR_2 = 0.0783$, and GOF = 1.015. Crystal data for $[\text{Mn}(2,3\text{-Me}_2\text{-QMTC})_2]_\infty$: formula $\text{C}_{22}\text{H}_{16}\text{Mn}_3\text{O}_{10}$, fw = 605.17, orthorhombic, space group $P2_12_12_1$, $a = 11.4061(6) \text{ \AA}$, $b = 12.0915(6) \text{ \AA}$, $c = 17.9405(9) \text{ \AA}$, $V = 2474.3(2) \text{ \AA}^3$, $Z = 4$, $\rho_{\text{calcd}} = 1.625 \text{ g cm}^{-3}$, $\mu = 1.560 \text{ mm}^{-1}$, $F(000) = 1212$, θ range 2.12–28.32°, 320 variables refined with 6142 independent reflections to final R indices [$I > 2\sigma(I)$] of $R_1 = 0.0494$ and $wR_2 = 0.0828$, and GOF = 0.983. Crystal data for $[\text{Mn}(2,3\text{-Me}_2\text{-QMTC})_2 \cdot \text{MeOH}]_\infty$: formula $\text{C}_{23}\text{H}_{20}\text{Mn}_3\text{O}_{11}$, fw = 637.21, orthorhombic, space group $P2_12_12_1$, $a = 11.2244(7) \text{ \AA}$, $b = 12.1179(7) \text{ \AA}$, $c = 18.4937(11) \text{ \AA}$, $V = 2515.4(3) \text{ \AA}^3$, $Z = 4$, $\rho_{\text{calcd}} = 1.683 \text{ g cm}^{-3}$, $\mu = 1.542 \text{ mm}^{-1}$, $F(000) = 1284$, θ range 2.01–25.04°, 339 variables refined with 4457 independent reflections to final R indices [$I > 2\sigma(I)$] of $R_1 = 0.0277$ and $wR_2 = 0.0733$, and GOF = 1.072.